



OPEN

Momentum dependent d_{xz}/yz band splitting in LaFeAsO

S. S. Huh^{1,2}, Y. S. Kim^{1,2}, W. S. Kyung^{1,2}, J. K. Jung^{1,2}, R. Kappenberger³, S. Aswartham³, B. Büchner^{3,4}, J. M. Ok^{5,6}, J. S. Kim^{5,6}, C. Dong^{7,8}, J. P. Hu^{7,8}, S. H. Cho⁹, D. W. Shen⁹, J. D. Denlinger¹⁰, Y. K. Kim^{11,12} & C. Kim^{1,2}✉

The nematic phase in iron based superconductors (IBSs) has attracted attention with a notion that it may provide important clue to the superconductivity. A series of angle-resolved photoemission spectroscopy (ARPES) studies were performed to understand the origin of the nematic phase. However, there is lack of ARPES study on LaFeAsO nematic phase. Here, we report the results of ARPES studies of the nematic phase in LaFeAsO. Degeneracy breaking between the d_{xz} and d_{yz} hole bands near the Γ and M point is observed in the nematic phase. Different temperature dependent band splitting behaviors are observed at the Γ and M points. The energy of the band splitting near the M point decreases as the temperature decreases while it has little temperature dependence near the Γ point. The nematic nature of the band shift near the M point is confirmed through a detwin experiment using a piezo device. Since a momentum dependent splitting behavior has been observed in other iron based superconductors, our observation confirms that the behavior is a universal one among iron based superconductors.

The discovery of iron based superconductors (IBS) over a decade ago brought renewed interest in high T_C superconductivity research^{1,2}. In addition to the superconductivity itself, its various phases have attracted much attention due to their possible relation to superconductivity. Among these phases, the nematic phase, a rotational symmetry broken state in the electronic structure, has been intensively studied as it also occurs in other unconventional superconductors³. Moreover, the divergent nematic susceptibility at the optimal doping suggests that the nematic fluctuation may play an important role in the formation of the Cooper pairs in IBS^{4,5}. Therefore, understanding the origin of the nematic phase can be a key to unraveling the mechanism of the unconventional superconductivity in IBS.

A number of angle-resolved photoemission spectroscopy (ARPES) experiments have been conducted to investigate the rotational symmetry broken electronic states. However, interpretations of experimental data differ from each other, making the origin of the nematic phase a more controversial issue. Various scenarios were proposed as the origin of the nematic phase based on ARPES results, such as simple Ferro-orbital order^{6,7}, d -wave bond order⁸, unidirectional nematic bond order⁹, and sign reversal order¹⁰. Among various candidates, the instability of the momentum dependent band splitting which is commonly observed in FeSe, NaFeAs and BaFe₂As₂ is favored as the true origin of the nematic phase^{11–13}.

In resolving such issue, confirming if the behavior of the nematic electronic structure is universal among IBS should be an important step. Despite the intensive research on the nematic phase^{14,15}, there is a lack of ARPES study on the nematic phase of LaFeAsO^{16,17} even though it is the first IBS that was discovered. Therefore,

¹Center for Correlated Electron Systems, Institute for Basic Science (IBS), Seoul 08826, Republic of Korea. ²Department of Physics and Astronomy, Seoul National University (SNU), Seoul 08826, Republic of Korea. ³Leibniz Institute for Solid State and Materials Research, IFW-Dresden, 01069 Dresden, Germany. ⁴Institute of Solid State Physics, TU Dresden, 01069 Dresden, Germany. ⁵Center for Artificial Low Dimensional Electronic Systems, Institute of Basic Science, Pohang 790-784, Republic of Korea. ⁶Department of Physics, Pohang University of Science and Technology, Pohang 790-784, Republic of Korea. ⁷Beijing National Laboratory for Condensed Matter Physics, Institute of Physics, Chinese Academy of Sciences, Beijing 100190, People's Republic of China. ⁸Collaborative Innovation Center of Quantum Matter, Beijing, People's Republic of China. ⁹State Key Laboratory of Functional Materials for Informatics, Shanghai Institute of Microsystem and Information Technology (SIMIT), Chinese Academy of Sciences, Shanghai 200050, People's Republic of China. ¹⁰Advanced Light Source, Lawrence Berkeley National Laboratory, Berkeley, CA 94720, USA. ¹¹Department of Physics, Korea Advanced Institute of Science and Technology, Daejeon 34141, Republic of Korea. ¹²Graduate School of Nanoscience and Technology, Korea Advanced Institute of Science and Technology, Daejeon 34141, Republic of Korea. ✉email: changyoung@snu.ac.kr

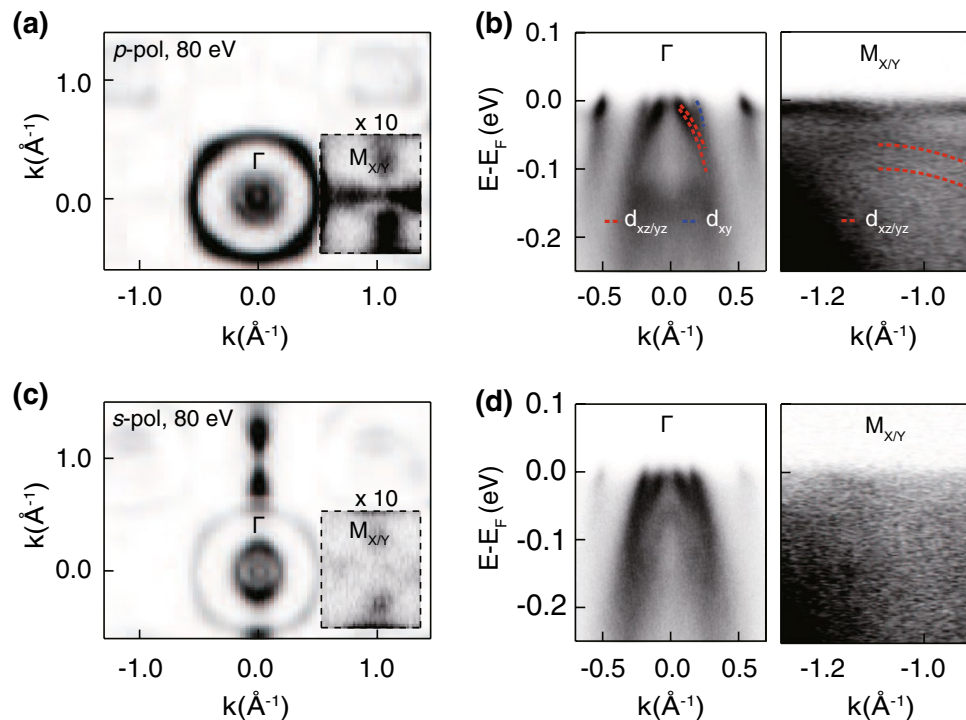


Figure 1. Angle-resolved photoemission spectroscopy (ARPES) measurements on LaFeAsO. (a) Fermi surface map taken with 80 eV and *p*-polarized light. The inset shows the intensity near the *M* point multiplied by 10 to show the details. (b) Corresponding band structure at the Γ and *M* points along the Γ -*M* direction. The red and blue dashed line indicate dispersions of $d_{xz/yz}$ and d_{xy} bands, respectively. (c) and (d) Similar measurements but with *s*-polarized light. All the data were taken at 30 K.

investigating electronic structure of the LaFeAsO nematic phase is an important step towards finding the origin of the nematic phase. In this work, we performed temperature dependent ARPES experiments on twinned and detwinned LaFeAsO crystals. The results show a nematic behavior similar to other IBS: finite near the *M* point but very small near the Γ point^{11–13}. Our observation of the momentum dependent nematic band splitting establishes a universal nematic behavior in IBS.

Results

Electronic structure of LaFeAsO Fig. 1a, c show Fermi surface maps of LaFeAsO taken with *p*- and *s*-polarized 80 eV light, respectively. Considering all the features of the two Fermi surface maps taken with different polarizations, we determine that the Fermi surface consists of three circular pockets around the Γ point and two peanut like pockets around the *M* point. Due to the low intensity near the *M* point, the intensity of the Fermi surface near the *M* point is multiplied by 10 and depicted in the inset. The observed Fermi surface topology is consistent with that from previous ARPES studies on LaFeAsO^{16–19}. Band structures near Γ and *M* are shown in Fig. 1b,d for *p*- and *s*-polarizations, respectively. Shown in Fig. 1b are the band dispersions as well as their orbital characters, determined based on tight binding calculation (see Supplementary Note 1). It is noteworthy that the bands which cannot be identified with the calculation results are surface states.

Temperature evolution of the electronic structure. We performed temperature dependent experiments presented to gain more information. Experiments were done 1 h after cleaving the sample at 30 K to remove the surface reconstruction effect¹⁷. The temperature evolution of d_{xz}/d_{yz} splitting near the Γ point can be seen in the high symmetry cut and its second derivative data shown in Fig. 2a,b, respectively. Temperature dependent high symmetry cut data shows that the band dispersions around the Γ point hardly change except the thermal broadening. That is, d_{xz}/d_{yz} hole band splitting near Γ , as indicated by the red dashed lines, appears to remain almost unchanged over the temperature range we studied. The energy splitting size may be obtained from the temperature dependent energy distribution curves (EDCs) of the second derivative data in Fig. 2c. The EDCs are from $k = 0.19 \text{ \AA}^{-1}$ as indicated by the yellow dotted line in Fig. 1b (Detailed analysis is described in Supplementary Note 2). Peak positions of d_{xz} and d_{yz} hole bands are indicated by the arrows. The band splitting at 30 K is about 50 meV and changes very little with the temperature, remaining finite even above T_S . That is, the d_{xz}/d_{yz} hole band splitting near the Γ point is not sensitive to the nematic phase transition.

In previous studies on other IBS, the d_{xz}/d_{yz} hole band splitting near the *M* point has been intensively studied because of its large temperature dependence^{6–8,10–12,17}. For that reason, we also focus on the temperature dependence of the electronic structure near the *M* point. Measurements were done with 21.2 eV photon energy where the cross section is higher for *M*. Temperature dependent data and their second derivatives are plotted in Fig. 2d,e. Split d_{xz} and d_{yz} hole bands are observed at low temperatures as indicated by red dashed lines. In

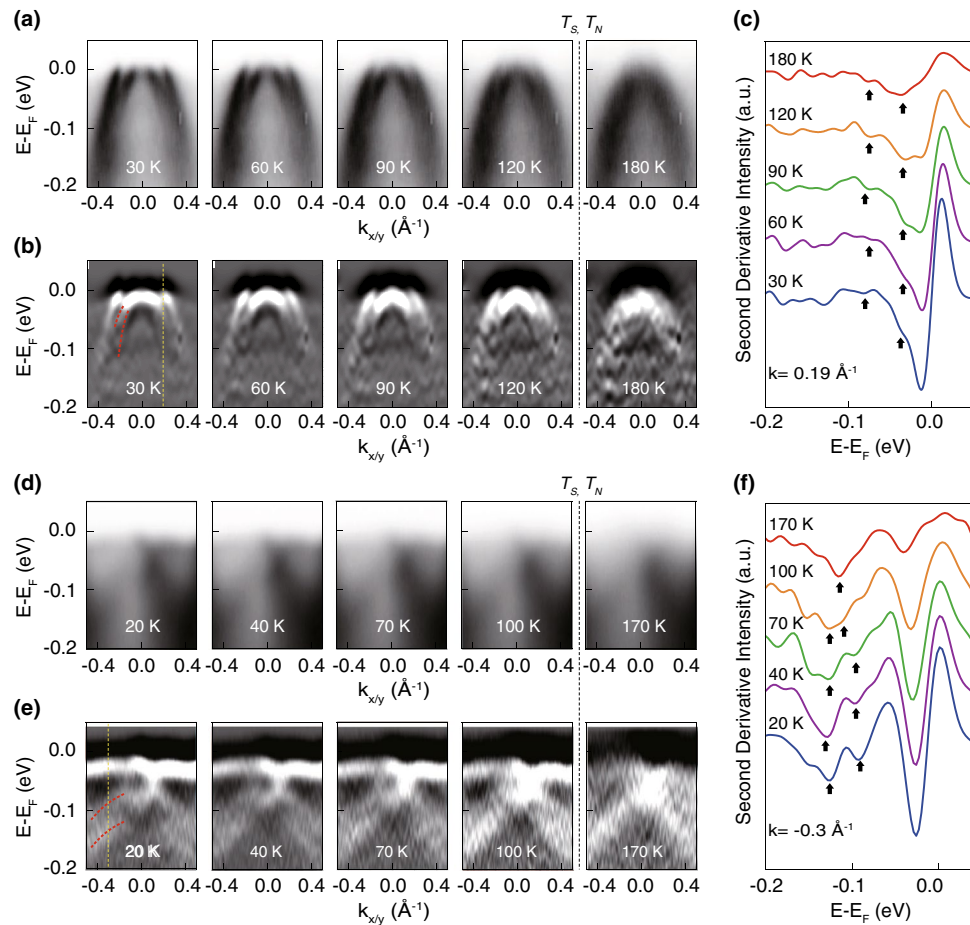


Figure 2. Temperature evolution of the electronic structure. **(a)** Temperature dependent ARPES data and **(b)** its second derivative near the Γ point taken with 80 eV photon. The red dashed lines indicate dispersions of $d_{xz/yz}$ bands. **(c)** Temperature dependent energy distribution curves (EDCs) at $k = 0.19 \text{ \AA}^{-1}$, indicated by the yellow dashed line in Fig. 2b. Peak positions of d_{xz} and d_{yz} are indicated by black arrows. **(d)** Temperature dependent ARPES data and **(e)** its second derivative data near the M point taken with 21.2 eV photon energy, for which the cross section is higher. **(f)** Temperature dependent EDCs at $k = -0.3 \text{ \AA}^{-1}$, indicated by the yellow dashed line in (e).

contrast to the temperature independent behavior near the Γ point, the splitting between the two hole bands gradually decreases as the temperature increases. The two bands finally merge each other to a single band above T_S . The temperature dependence of band splitting may be observed more clearly in the EDCs of second derivative data at $k = -0.3 \text{ \AA}^{-1}$ in Fig. 2f. The splitting energy at a low temperature is about 40 meV and vanishes above the nematic phase transition temperature T_S .

Electronic structures of twinned and detwinned LaFeAsO. Even though the temperature dependent behavior strongly indicates that the band splitting near M is due to the nematic order, a true confirmation of the nematic nature should come from observation of dependent shift. In previous ARPES studies on detwinned IBS^{6,7,11}, nematic band shift has been observed in which the d_{yz} (d_{xz}) hole band from a single domain shifts upward (downward) along $\Gamma-M_X$ (M_Y). Such band shifts lead to a simple energy splitting between the d_{xz} and d_{yz} hole bands in the twinned sample due to the mixed signals from two perpendicularly arranged domains in the nematic phase. It is reasonable to speculate that observed band splitting near the M point in our data is also from the superposition of the d_{yz} hole band along $\Gamma-M_X$ and the d_{xz} hole band along $\Gamma-M_Y$ in LaFeAsO. This can be clarified through detwin experiments.

Detwinning was done by using a piezo stack based strain device which was adopted in previous FeSe studies¹¹. Tensile strain is transmitted to the sample glued to the piezo device when voltage is applied to the device. In our experiment, we applied 150 V to the piezo device at 200 K and cooled down the sample. Figure 3a shows the experimental geometry for the experiment. Band dispersion near the M_Y point along the k_x -direction in twinned and detwinned samples are presented in Fig. 3b,c, respectively. In the detwin data, only the upper hole band (d_{yz}) without the lower hole band (d_{xz}) is seen in comparison to the twin data. Note that the band dispersion in this experimental geometry is the same as the one obtained along the k_x -direction at M_X due to the band folding; M_Y was chosen because the intensity is higher. Therefore, considering the normal state band dispersions as well as our detwin experiment result, we conclude that LaFeAsO also has nematic band shifts similar to other IBS²⁰.

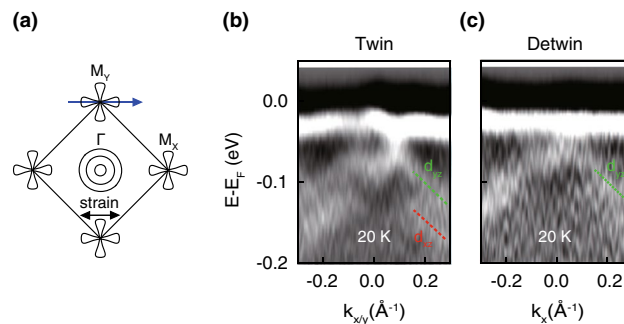


Figure 3. Electronic structures of twinned and detwinned LaFeAsO at M point. **(a)** Schematic illustration of experimental geometry. High symmetry cut of the **(b)** twinned and **(c)** detwinned sample along k_x -direction near the M_Y point. The red and green dashed line indicated dispersion of d_{xz} and d_{yz} band, respectively. Tensile strain is transmitted to sample by applying 150 V to the piezo strain device.

Discussion

The discovery of the nematic band shift near M was taken to be an evidence for a Ferro-orbital order which in turn was considered to be the origin of the nematic phase. It is theoretically suggested that a nearly constant band splitting is expected in the entire Brillouin zone when Ferro-orbital order exists^{21,22}. However, ARPES results show that the band splitting has momentum dependence for all IBS systems including LaFeAsO, which excludes the Ferro-orbital scenario as the origin. Rather than the Ferro-orbital order, the instability for the observed universal momentum dependent band splitting should be the true origin of the nematic phase. There are proposals such as different form of orbital degree of freedom²³, Pomeranchuk instability²⁴ and spin degree of freedom^{25–27} that require momentum dependence. Finding out which one of these is truly responsible for the nematic phase requires full understanding of the nematic electronic structure. As proposed very recently^{11,28}, in addition to consideration of d_{xz} and d_{yz} hole bands, evolution of d_{xz}/d_{yz} electron bands, spin orbit coupling and role of d_{xy} band should be elucidated to resolve the issue.

Methods

High quality LaFeAsO single crystals were synthesized by using solid state crystal growth technique²⁹. The structural and magnetic transition temperatures (T_S and T_N) were found to be around 145 and 127 K, respectively^{29,30}. ARPES measurements were performed at the beam line 4.0.3 of the Advanced Light source (ALS) and beam line 03U of the Shanghai Synchrotron Radiation Facility (SSRF), and also with a lab-based system at Seoul National University (SNU). Piezo detwin ARPES experiments were performed with the system at SNU. 150 V bias voltage was applied to the piezo device to detwin samples. All spectra were acquired with VG-Scienta electron analyzers. The samples were cleaved in an ultrahigh vacuum better than 5×10^{-11} torr. To minimize the aging effect, all the data were taken within 8 h after cleave.

Received: 3 August 2020; Accepted: 16 October 2020

Published online: 09 November 2020

References

- Kamihara, Y., Watanabe, T., Hirano, M. & Hosono, H. Iron-based layered superconductor $\text{La}(\text{O}_{1-x}\text{F}_x)\text{FeAs}$ ($x=0.05\text{--}0.12$) with $T_C = 26$ K. *J. Am. Chem. Soc.* **130**, 3296 (2008).
- Paglione, J. & Greene, R. L. High-temperature superconductivity in iron-based materials. *Nat. Phys.* **6**, 645 (2010).
- Fernandes, R. M., Chubukov, A. V. & Schmalian, J. What drives nematic order in iron-based superconductors?. *Nat. Phys.* **10**, 97 (2014).
- Chu, J.-H., Kuo, H.-H., Analytis, J. G. & Fisher, I. R. Divergent nematic susceptibility in an iron arsenide superconductor. *Science* **337**, 710–712 (2012).
- Kuo, H.-H. *et al.* Ubiquitous signatures of nematic quantum criticality in optimally doped Fe-based superconductors. *Science* **352**, 958–962 (2016).
- Yi, M. *et al.* Symmetry-breaking orbital anisotropy observed for detwinned $\text{Ba}(\text{Fe}_{1-x}\text{Co}_x)_2\text{As}_2$ above the spin density wave transition. *Proc. Natl. Acad. Sci. USA* **108**, 6878–6883 (2011).
- Yi, M. *et al.* Electronic reconstruction through the structural and magnetic transitions in detwinned NaFeAs. *New J. Phys.* **14**, 073019 (2012).
- Zhang, P. *et al.* Observation of two distinct d_{xz}/d_{yz} band splittings in FeSe. *Phys. Rev. B* **91**, 214503 (2016).
- Watson, M. D. *et al.* Evidence for unidirectional nematic bond ordering in FeSe. *Phys. Rev. B* **94**, 201107 (2016).
- Suzuki, Y. *et al.* Momentum-dependent sign inversion of orbital order in superconducting FeSe. *Phys. Rev. B* **92**, 205117 (2015).
- Huh, S. S. *et al.* Absence of Y-pocket in 1-Fe Brillouin zone and reversed orbital occupation imbalance in FeSe. *Commun. Phys.* **3**, 52 (2020).
- Pfau, H. *et al.* Momentum dependence of the nematic order parameter in iron-based superconductors. *Phys. Rev. Lett.* **123**, 066402 (2019).
- Ge, Q. Q. *et al.* Anisotropic but nodeless superconducting gap in the presence of spin-density wave in iron-pnictide superconductor $\text{NaFe}_{1-x}\text{Co}_x\text{As}$. *Phys. Rev. X* **3**, 011020 (2013).
- Li, H.-F. *et al.* Phase transitions and iron-ordered moment form factor in LaFeAsO. *Phys. Rev. B* **82**, 064409 (2010).

15. Fang, C., Yao, H., Tsai, W.-F., Hu, J. & Kivelson, S. A. Theory of electron nematic order in LaFeAsO. *Phys. Rev. B* **77**, 224509 (2008).
16. Yang, L. X. *et al.* Surface and bulk electronic structures of LaFeAsO studied by angle-resolved photoemission spectroscopy. *Phys. Rev. B* **82**, 104519 (2010).
17. Zhang, P. *et al.* Disentangling the surface and bulk electronic structures of LaOFeAs. *Phys. Rev. B* **94**, 104517 (2016).
18. Charnukha, A. *et al.* Interaction-induced singular Fermi surface in a high-temperature oxypnictide superconductor. *Sci. Rep.* **5**, 10392 (2015).
19. Lu, D. H. *et al.* Electronic structure of the iron-based superconductor LaOFeP. *Nature (London)* **455**, 81 (2008).
20. Onari, S., Yamakawa, Y. & Kontani, H. Sign-reversing orbital polarization in the nematic phase of FeSe due to the C_2 symmetry breaking in the self-energy. *Phys. Rev. Lett.* **116**, 227001 (2016).
21. Lee, C. C., Yin, W. G. & Ku, W. Ferro-orbital order and strong magnetic anisotropy in the parent compounds of iron-pnictide superconductors. *Phys. Rev. Lett.* **103**, 267001 (2009).
22. Chen, C.-C. *et al.* Orbital order and spontaneous orthorhombicity in iron pnictides. *Phys. Rev. B* **82**, 100504(R) (2010).
23. Li, T. & Su, Y. Driving force of the orbital-relevant electronic nematicity in Fe-based superconductors. *J. Phys. Condens. Matter.* **29**, 425603 (2017).
24. Chubukov, A. V., Khodas, M. & Fernandes, R. M. Magnetism, superconductivity, and spontaneous orbital order in iron-based superconductors: Which comes first and why?. *Phys. Rev. X* **6**, 041045 (2016).
25. Fanfarillo, L. *et al.* Orbital-dependent Fermi surface shrinking as a fingerprint of nematicity in FeSe. *Phys. Rev. B* **94**, 155138 (2016).
26. Wang, F., Kivelson, S. A. & Lee, D.-H. Nematicity and quantum paramagnetism in FeSe. *Nat. Phys.* **11**, 959 (2015).
27. Fernandes, R. M. *et al.* Effects of nematic fluctuations on the elastic properties of iron arsenide superconductors. *Phys. Rev. Lett.* **105**, 157003 (2010).
28. Yi, M. *et al.* Nematic energy scale and the missing electron pocket in FeSe. *Phys. Rev. X* **9**, 041049 (2019).
29. Kappenberger, R. *et al.* Solid state single crystal growth of three-dimensional faceted LaFeAsO crystals. *J. Cryst. Growth* **483**, 9 (2018).
30. Materne, P. *et al.* Microscopic phase diagram of LaFeAsO single crystals under pressure. *Phys. Rev. B* **98**, 174510 (2018).

Acknowledgements

This work is supported by IBS-R009-G2 through the IBS Center for Correlated Electron Systems. Theoretical part was supported by grants from CAS (XDB07000000). Part of this research used Beamline 03U of the Shanghai Synchrotron Radiation Facility, which is supported by ME2 project under contract No. 11227902 from National Natural Science Foundation of China. The work at Pohang University of Science and Technology (POSTECH) was supported by IBS (no. IBS-R014-D1) and the NRF through the SRC (No. 2018R1A5A6075964) and the Max Planck-POSTECH Center (No. 2016K1A4A4A01922028). The work at IFW was supported by the (DFG) through the Priority Program SPP 1458. The work at Korea Advanced Institute of Science and Technology (KAIST) was supported by NRF through National R & D Program (No. 2018K1A3A7A09056310), Creative Materials Discovery Program (No. 2015M3D1A1070672), Basic Science Resource Program (No. 2017R1A4A1015426, No. 2018R1D1A1B07050869), and the internal R&D program at KAERI. The Advanced Light Source is supported by the Office of Basic Energy Sciences of the US DOE under Contract No. DE-AC02-05CH11231.

Author contributions

R..K, S.A., B.B., J.M.O. and J.S.K. grew the crystals. S.S.H., Y.S.K., W.S.K. and S.H.C. carried out the ARPES measurements with the support from J.K.J., J.D.D., D.W., C.D. and J.P.H. performed the tight-binding analysis. S.S.H. analysed the ARPES data with Y.K.K. and C.K. S.S.H. and C.K. wrote the manuscript. All authors discussed the results and reviewed the manuscript. C.K. was responsible for the overall research direction and planning.

Competing interests

The authors declare no competing interests.

Additional information

Supplementary information is available for this paper at <https://doi.org/10.1038/s41598-020-75600-w>.

Correspondence and requests for materials should be addressed to C.K.

Reprints and permissions information is available at www.nature.com/reprints.

Publisher's note Springer Nature remains neutral with regard to jurisdictional claims in published maps and institutional affiliations.



Open Access This article is licensed under a Creative Commons Attribution 4.0 International License, which permits use, sharing, adaptation, distribution and reproduction in any medium or format, as long as you give appropriate credit to the original author(s) and the source, provide a link to the Creative Commons licence, and indicate if changes were made. The images or other third party material in this article are included in the article's Creative Commons licence, unless indicated otherwise in a credit line to the material. If material is not included in the article's Creative Commons licence and your intended use is not permitted by statutory regulation or exceeds the permitted use, you will need to obtain permission directly from the copyright holder. To view a copy of this licence, visit <http://creativecommons.org/licenses/by/4.0/>.

© The Author(s) 2020